A Neural Network Approach to Estimate Tropical Cyclone Heat Potential in the Indian Ocean

M. M. Ali, P. S. V. Jagadeesh, I.-I. Lin, and Je-Yuan Hsu

***Abstract*—The tropical cyclone heat potential (TCHP) or the available upper ocean thermal energy is one of the critical factors in controlling the intensity of cyclones. Given the devastating impacts Indian Ocean cyclones could bring (e.g., the "killer cyclone" Nargis in 2008, which caused more than 130 000 deaths), there is a pressing need to obtain reliable and more accurate TCHP estimates over the Indian Ocean to improve the cyclone track and intensity predictions. Using more than 25 000 *in situ* subsurface temperature profiles during 1997–2007, this research explores the possibility of developing an artificial neural network (ANN) model to derive TCHP in the Indian Ocean using satellite-derived sea surface height anomalies, sea surface temperature, and climatological depth of 26 °C isotherm. The estimations have been validated using more than 8000 independent *in situ* profiles during 2008–2009. The root-mean-square error and the scatter index of this validation data sets are 14.6 kJ/cm^2 and 0.2, respectively. Comparison of the estimations from a two-layer reduced gravity model and from a multiple regression method confirms the superiority of the ANN approach over other methods.**

***Index Terms*—Artificial neural networks, Indian Ocean, Tropical cyclone heat potential.**

I. Introduction

ENERGY from the oceans is one of the critical factors influencing the intensification of tropical cyclones (TCs). DeMaria and Kaplan [1] and DeMaria [2] studied the relationship between cyclone intensity (CI) and sea surface temperature (SST). After the sudden intensification of Hurricane Opal when passing over a warm oceanic feature [3], the role played by the upper ocean thermal structure has taken prominence in cyclone intensification studies. Goni and Trinanes [4], DeMaria *et al.* [5], Wada and Usui [6], Lin *et al.* [7]–[9], Mainelli *et al.* [10], and Wada and Chan [11] emphasized the importance of tropical cyclone heat potential (TCHP) in CI predictions. Ali *et al.* [12], [13] studied the role of oceanic eddies on cyclone intensification and track in the North Indian Ocean. In addition to SST, TCHP, which is defined as the heat content of the ocean integrated from surface to the 26 °C isotherm [14], has been studied in regard to its possible relations with TC intensity [4], [6]–[9] and [15]. Shay *et al.* [3] and Scharroo *et al.* [16] suggested that, in addition to high SST, high TCHP is also required for intensifying cyclones. Lin *et al.* [9] explored the role of high TCHP played in the rapid intensification of the "killer" cyclone Nargis (2008) in the North Indian Ocean. Soon after its rapid intensification over the high-TCHP region, Nargis had landfall and resulted in more than 130 000 deaths [9]. Since the Indian coast has highly varying bathymetry, even a slight error in predicting the landfall point and intensity could lead to a totally different storm surge height.

Given the importance of TCHP in the intensity of Indian Ocean cyclones, it is necessary to improve the accuracy of the TCHP estimations to assist CI forecast and analysis [9], [17]. The spatially and temporally limited availability of *in situ* hydrographic observations constrains the estimation and monitoring of TCHP on a regular basis, particularly over regions of TC activity. Since the sea surface height anomaly (SSHA) is strongly correlated with the thermal structure of the upper ocean [3], [18], [19], TCHP can be estimated from this parameter over finer spatial and temporal scales. Details of the estimation of TCHP from climatological temperature profiles, SST, and SSHA observations using a two-layer reduced gravity model are given in [3], [4], [18], and [20]. In addition to this model, artificial neural networks (ANNs) are another possible method to derive TCHP based on altimeter observations. The ANN technique has proved its capability in the estimation of various oceanic parameters and subsurface information such as mixed and sonic layer depths from the surface observations [21]–[24].

In this paper, we developed an ANN technique to estimate TCHP using about 25 000 *in situ* temperature profiles, climatological depth of 26 °C isotherm ($D26_c$), and the collocated SST and SSHA observations over the North Indian Ocean spanning 10 °S–25 °N latitude and 40 °E–100 °E longitude. SSHA represents the subsurface thermal structure, whereas SST represents the heat energy at the surface. $D26_c$ provides the climatological background over which changes take place. We validated the results using more than 8000 independent *in situ* observations. We also computed TCHP from a widely used two-layer reduced gravity model and with the multiple regression method to conclude the superiority of the ANN technique.

II. Data and Methodology

The data sets used in this study during 1997–2009 are: 1) quality-controlled *in situ* temperature profiles available from all the platforms (e.g., expendable bathythermographs, profiling floats, conductivity–temperature–depth profiles, and moorings) in the World Ocean Database [25]; 2) weekly merged SSHA product at $1/3^\circ \times 1/3^\circ$ resolution obtained from AVISO

Manuscript received February 2, 2012; accepted February 27, 2012.

M. M. Ali is with the Atmosphere and Ocean Sciences Group, National Remote Sensing Centre, Hyderabad 500037, India.

P. S. V. Jagadeesh is with the Naval Physical and Oceanographic Laboratory, Kochi 682021, India.

I.-I. Lin and J.-Y. Hsu are with the Department of Atmospheric Sciences, National Taiwan University, Taipei 106, Taiwan.

Digital Object Identifier 10.1109/LGRS.2012.2190491

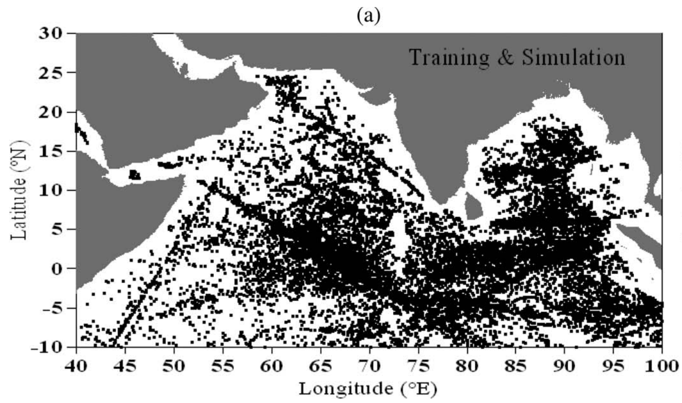

Fig. 1. *In situ* observations used (a) in developing the ANN model and (b) for validation.

(Archiving, Validation and Interpretation of Satellite Oceanographic data); and 3) three-day daily average SST at $0.25° \times 0.25°$ resolution from TMI (TRMM (Tropical Rainfall Monitoring Mission) Microwave Imager). The location of *in situ* data used in developing the ANN model (during 1997–2007) and those used for validating the results (during 2008–2009) are shown in Fig. 1.

Since TCHP is defined as the integrated heat content from surface to the depth of 26 °C isotherm, all the profiles with SST equal to or less than 26 °C are discarded. The depth of 26 °C is linearly interpolated if a measurement at this temperature is not available. TCHP (kJ/cm^2) is estimated from all the available temperature profiles following the equation [14]:

$$\text{TCHP} = \rho C_p \int_0^{D26} (T - 26) dZ \tag{1}$$

where ρ is the average density of the sea water, C_p is the specific heat capacity at constant pressure, T is the temperature (°C) at each layer of dZ thickness, and $D26$ is the depth of 26 °C isotherm.

SSHA and SST values are interpolated to the corresponding *in situ* location and period using a simple linear interpolation technique. Monthly climatology of $D26_c$, at $1° \times 1°$ spatial resolution, is estimated from World Ocean Atlas 2009 [26]. The $D26_c$ value is also assigned to the collocated observations depending upon the grid and month of the *in situ* observations.

A. ANN Approach

ANN is a massive parallel-distributed computer model consisting of simple processing units called artificial neurons that are the basic functioning units. The neural network formulation is based on the fact that any parameterization of a process can be considered as continuous (with finite discontinuities) mapping (input versus output vector dependence), which is analogous to atmospheric and ocean models with forcing and response. ANN has been widely used in various meteorological, oceanographic, atmospheric studies, and satellite remote sensing retrievals [21]–[24], [27]–[32].

The ANN analysis requires three data sets: 1) training; 2) verification; and 3) validation. The training data set trains the ANN model through several iterations. The verification data set is used to validate the model during this process so that the model does not over-fit during training. At this stage, the ANN verifies whether the model developed for the training data set holds good outside the training data range, in terms of root-mean-square error (RMSE), and applies a midterm correction, in case required. Thus, the training and verification data sets are used to develop the model. The developed model is then stored and used for estimating the output using the input parameters from the data set marked for validation.

In the present analysis, we used multilayer perceptrons, which are feedforward neural networks, with one input layer, three hidden layer, and one output layer. We tried several models, and the present topology is selected based upon the least error. The input (independent) parameters are SSHA, SST, and $D26_c$. The dependent parameter (output) is the TCHP estimated from the *in situ* observations. Out of the 35 165 observations, we used about 34% of the data set (11 812 observations) during 1997–2004 for training the ANN model, about 42% (14 916 sets) during 2005–2007 for verification, and 24% (8437 sets) during 2008–2009 for validation of the predicted results. Thus, the 24% of the data, marked for validation, were held back and were not used in training the model.

B. TCHP Derivation from The Two-Layer Reduced Gravity Model

We estimated TCHP, for the validation data set, by a two-layer reduced gravity model originally proposed by Goni *et al.* [18] and Shay *et al.* [3]. In this procedure, the depth of 20 °C isotherm ($D20$) is estimated from SSHA by the two-layer scheme as

$$D20(x,y,t) = \overline{D20}(x,y) + \frac{\rho_2(x,y)}{\rho_2(x,y) - \rho_1(x,y)} \eta'(x,y,t) \tag{2}$$

where, $\overline{D20}$ is the climatological depth of 20 °C isotherm ($D20$) obtained from the temperature analysis of World Ocean Atlas, ρ_1 and ρ_2 are the density of the upper (surface to $D20$) and lower layer ($D20$ to ocean bottom), and η' is SSHA. $D26$ is computed from derived $D20$ by using a climatological ratio between $D26$ and $D20$. Once the depth of 26 °C is estimated and SST obtained from satellite observations, the TCHP is the

TABLE I
STATISTICS OF THE TRAINING, VERIFICATION, AND VALIDATION DATA SETS

Case	No. of Obs.	*In situ* TCHP (kJ/cm^2)				Estimated TCHP (kJ/cm^2)					
		Min	Max	Mean	SD	AEM	AMPE	ESD	SDR	RMSE	SI
Training	11812	6.3	199.1	69.3	25.4	11.9	17	9.5	0.37	15.2	0.22
Verification	14916	4.0	175.7	76.4	25.2	11.9	16	9.1	0.36	15.2	0.20
Validation	8437	4.4	172.2	73.6	26.0	11.6	16	8.9	0.34	14.6	0.20

excess heat contained above the 26 °C isotherm. The details of this computation are given in [18]. Momin *et al.* [33] also used a similar approach to get the heat content up to $D20$ using a regression relationship between SST and the upper layer temperature based on historical Argo profiles.

C. TCHP Derivation From Multiple Regression Method

Using the training and selection data sets described in Section II-A (26 728 observations), the following multiple regression equation is obtained:

$$\mathrm{TCHP} = -245.256 + D26_c * 0.533 + \mathrm{SSHA} * 0.369 + \mathrm{SST} * 0.279 \quad (3)$$

where $D26_c$ is in m, SSHA in cm, and SST in °C.

TCHP values have been estimated using the input parameters of the validation data set (8437 observations) using (3), and the results were compared with the *in situ* estimations.

III. VALIDATION

Absolute error mean (AEM: average of absolute differences between estimated and *in situ* values), absolute mean percentage error (AMPE: the percentage of the AEM to data mean), standard deviation errors in estimations (ESD), standard deviation (SD) ratio (SDR: ratio of ESD to data SD), RMSE, and scatter index (SI: ratio of RMSE to mean of *in situ* observations) for the training, verification, and validation data sets are shown in Table I.

In this analysis, the AEM for the validation set is 11.6 kJ/cm^2 for a range of 4.4–172.2 kJ/cm^2 with a mean value of 73.6 kJ/cm^2. The RMSE for this data set is 14.6 kJ/cm^2 with an SDR of 0.34 and an SI of 0.2, indicating the accuracy of the estimations (see Table I). The scatter between the *in situ* and ANN-estimated TCHP values is reasonably good with an R of 0.81 (see Fig. 2). The histogram analysis (figure not shown) of the data reveals that 80% of the estimations lie within ± 20 kJ/cm^2. Comparing the 8329 *in situ* and altimeter-derived TCHP observations during 2002–2005, Mainelli *et al.* [10] obtained an absolute error mean of 13.5 kJ/cm^2 in the Atlantic Ocean for a range of 0–150 kJ/cm^2 with a mean value of 41 kJ/cm^2. Pun *et al.* [34] validated the altimetry-derived upper ocean thermal structure in the western North Pacific Ocean and obtained an RMSE of about 30 kJ/cm^2. Nagamani *et al.* [35] validated satellite-derived TCHP observations by National Oceanic and Atmospheric Administration (NOAA)/Atlantic Oceanographic and Meteorological laboratory (AOML) with *in situ* observations over the North Indian Ocean during 1993–2009. They obtained an RMSE of 20.9 kJ/cm^2.

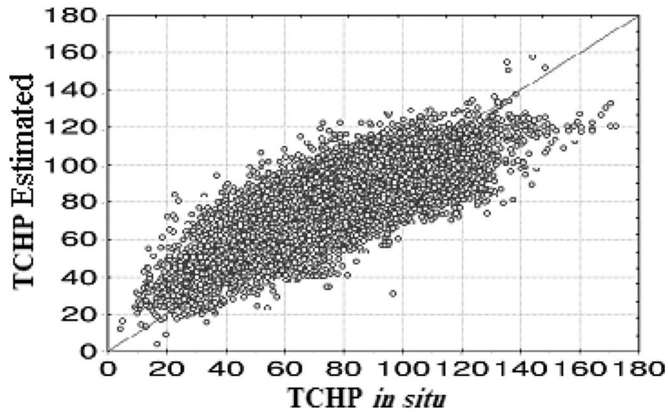

Fig. 2. Scatter between the *in situ* and satellite-estimated TCHP (kJ/cm^2) by the ANN method.

The TCHP estimated from the two-layer reduced gravity model for the validation data set has an absolute error mean of 13.97 kJ/cm^2 with an RMSE of 17.88 kJ/cm^2. Similarly, the TCHP estimated from the multiple regression has an absolute error mean of 12.7 kJ/cm^2 and an RMSE of 16.34 kJ/cm^2. Comparison of the ANN estimations with the above results suggests that the satellite-derived TCHP using the ANN technique can be conveniently used to estimate this parameter with better accuracy compared with the two-layer reduced gravity model and the multiple regression method in the North Indian Ocean.

IV. SUMMARY AND CONCLUSION

TCHP is one of the critical factors in controlling the intensity of cyclones. In view of the limitations of the *in situ* temperature profiles, satellite-derived estimations of this parameter is the only solution to have a better spatial and temporal coverage in regions such as the Indian Ocean where devastating cyclones frequently occur. Regional validation of any satellite estimation is essential for an effective utilization. We estimated TCHP by 1) an ANN technique, 2) a two-layer reduced gravity model, and 3) a multiple regression technique and compared the estimations with the *in situ* observations. Out of the three methods, the ANN approach has given the best results. The results suggest the utility of the ANN technique in estimating TCHP with better accuracy in the North Indian Ocean that certainly, in turn, helps in improving the cyclone track and intensity predictions.

Acknowledgment

The authors would like to thank the CNES/AVISO team for providing the altimeter product, the Remote Sensing System for providing the SST data, and the National Oceanographic Data Center (NODC) under the U.S. National Oceanographic and Atmospheric Administration (NOAA) for providing the ocean depth–temperature profiles. They would also like to thank their respective centers for the support and encouragement and the three anonymous referees for their comments and suggestions. I.-I. Lin would like to thank the National Science Council of Taiwan.

References

[1] M. DeMaria and J. Kaplan, "Sea surface temperature and the maximum intensity of Atlantic tropical cyclones," *J. Climate*, vol. 7, no. 9, pp. 1324–1334, Sep. 1994.

[2] M. DeMaria, "A simplified dynamical system for tropical cyclone intensity prediction," *Mon. Weather Rev.*, vol. 137, no. 1, pp. 68–82, Jan. 2009.

[3] L. K. Shay, G. J. Goni, and P. G. Black, "Effects of a warm oceanic feature on Hurricane Opal," *Mon. Weather Rev.*, vol. 128, no. 5, pp. 1366–1383, May 2000.

[4] G. J. Goni and J. A. Trinanes, "Ocean thermal structure monitoring could aid in the intensity forecast of tropical cyclones," *EOS Trans. AGU*, vol. 84, no. 51, p. 573, 2003.

[5] M. DeMaria, M. Mainelli, L. K. Shay, J. A. Knaff, and J. Kaplan, "Further improvements to the Statistical Hurricane Intensity Prediction Scheme (SHIPS)," *Weather Forecast.*, vol. 20, no. 4, pp. 531–543, 2005.

[6] A. Wada and N. Usui, "Importance of tropical cyclone heat potential for tropical cyclone intensity and intensification in the western North Pacific," *J. Oceanogr.*, vol. 63, no. 3, pp. 427–447, Jun. 2007.

[7] I. I. Lin, C. C. Wu, and I.-F. Pun, "Upper ocean thermal structure and the western North Pacific category-5 typhoons—Part I: Ocean features and category-5 typhoons," *Mon. Weather Rev.*, vol. 136, no. 9, pp. 3288–3306, Sep. 2008.

[8] I. I. Lin, I.-F. Pun, and C.-C. Wu, "Upper ocean thermal structure and the western North Pacific category-5 typhoons Part II: Dependence on translation speed," *Mon. Weather Rev.*, vol. 137, no. .11, pp. 3744–3757, 2009.

[9] I. I. Lin, C.-H. Chen, I.-F. Pun, W. T. Liu, and C.-C. Wu, "Warm ocean anomaly, air sea fluxes, and the rapid intensification of tropical cyclone Nargis," *Geophys. Res. Lett.*, vol. 36, p. L03 817, Feb. 2009.

[10] M. Mainelli, M. DeMaria, L. K. Shay, and G. Goni, "Application of oceanic heat content estimation to operational forecasting of recent Atlantic category 5 hurricanes," *Weather Forecast.*, vol. 23, no. 1, pp. 3–16, 2008.

[11] A. Wada and J. C. L. Chan, "Relationship between typhoon activity and upper ocean heat content," *Geophys. Res. Lett.*, vol. 35, p. L17 603, Sep. 2008.

[12] M. M. Ali, P. S. V. Jagadeesh, and S. Jain, "Effects of eddies and dynamic topography on the Bay of Bengal cyclone intensity," *EOS, Trans. AGU*, vol. 88, no. 8, pp. 93–95, 2007.

[13] M. M. Ali, P. Sinha, S. Jain, and U. C. Mohanty, "Impact of sea surface height anomalies on cyclone track," *Nature Precedings*, 2007. DOI: 10.1038/npre.2007.1001.1.

[14] D. F. Leipper and D. Volgenau, "Hurricane heat potential of the Gulf of Mexico," *J. Phys. Oceanogr.*, vol. 2, no. 3, pp. 218–224, Jul. 1972.

[15] I. I. Lin, C. C. Wu, K. A. Emanuel, I. H. Lee, C. R. Wu, and I. F. Pun, "The interaction of supertyphoon Maemi (2003) with a warm ocean eddy," *Mon. Weather Rev.*, vol. 133, no. 9, pp. 2635–2649, 2005.

[16] R. Scharroo, W. H. F. Smith, and J. L. Lillibridge, "Satellite altimetry and the intensification of hurricane Katrina," *EOS Trans. AGU*, vol. 86, no. 40, p. 366, 2005.

[17] G. J. Goni and J. Knaff, "Tropical Cyclone Heat Potential ['In State of the Climate in 2008']," *Bull. Amer. Meteor. Soc.*, vol. 90, no. 8, pp. S54–S56, 2009.

[18] G. Goni, S. Kamholz, S. Garzoli, and D. Olson, "Dynamics of the Brazil–Malvinas Confluence based on inverted echo sounders and altimetry," *J. Geophy. Res*, vol. 101, pp. 16 273–16 289, 1996.

[19] J. K. Willis, D. Roemmich, and B. Cornuelle, "Interannual variability in upper-ocean heat content, temperature and thermosteric expansion on global scales," *J. Geophys. Res.*, vol. 109, p. C12 036, Dec. 2004.

[20] G. J. Goni, M. DeMaria, J. Knaff, C. Sampson, I. Ginis, F. Bringas, A. Mavume, C. Lauer, I.-I. Lin, M. M. Ali, P. Sandery, S. Ramos-Buarque, K. Kang, A. Mehra, E. Chassignet, and G. Halliwell, "Applications of satellite-derived ocean measurements to tropical cyclone intensity forecasting," *Oceanography*, vol. 22, no. 3, pp. 176–183, 2009.

[21] M. M. Ali, D. Swain, and R. A. Weller, "Estimation of ocean subsurface thermal structure from surface parameters: A neural network approach," *Geophys. Res. Lett.*, vol. 31, p. L20 308, Oct. 2004.

[22] S. Jain and M. M. Ali, "Estimation of sound speed profiles using artificial neural networks," *IEEE Geosci. Remote Sens. Lett.*, vol. 3, no. 4, pp. 467–470, Oct. 2006.

[23] D. Swain, M. M. Ali, and R. A. Weller, "Estimation of mixed-layer depth from surface parameters," *J. Mar. Res.*, vol. 64, no. 5, pp. 745–758, Sep. 2006.

[24] S. Jain, M. M. Ali, and P. N. Sen, "Estimation of sonic layer depth from surface parameters," *Geophys. Res. Lett.*, vol. 34, p. L17 602, Sep. 2007.

[25] D. R. Johnson, T. P. Boyer, H. E. Garcia, R. A. Locarnini, O. K. Baranova, and M. M. Zweng, "World ocean database 2009 documentation," NODC, Silver Spring, MD, NODC Internal Rep. 20, 2009, Ed. S. Levitus.

[26] R. A. Locarnini, A. V. Mishonov, J. I. Antonov, T. P. Boyer, H. E. Garcia, O. K. Baranova, M. M. Zweng, and D. R. Johnson, *World Ocean Atlas 2009*, S. Levitus, Ed. Washington, DC: NOAA Atlas, U.S. Government Printing Office, 2010.

[27] Q. H. Liu, C. Simmer, and E. Ruprecht, "Estimating longwave net radiation at sea surface from the Special Sensor Microwave/Imager (SSM/I)," *J. Appl. Meteor.*, vol. 36, no. 7, pp. 919–930, Jul. 1997.

[28] F. Chevallier, J.-J. Morcrette, F. Chéruy, and N. A. Scott, "Use of a neural-network-based longwave radiative transfer scheme in the EMCWF atmospheric model," *Q. J. R. Meteor. Soc.*, vol. 126, pp. 761–776, 2000.

[29] V. Krasnopolsky, D. V. Chalikov, and H. L. Tolman, "A neural network technique to improve computational efficiency of numerical oceanic models," *Ocean Model.*, vol. 4, no. 3/4, pp. 363–383, Jun. 2002.

[30] V. M. Krasnopolsky, M. S. Fox-Rabinovitz, and D. V. Chalikov, "New approach to calculation of atmospheric model physics: Accurate and fast neural network emulation of longwave radiation in a climate model," *Mon. Weather Rev.*, vol. 133, no. 5, pp. 1370–1383, May 2005.

[31] H. L. Tolman, V. M. Krasnopolsky, and D. V. Chalikov, "Neural network approximations for nonlinear interactions in wind wave spectra: Direct mapping for wind seas in deep water," *Ocean Model.*, vol. 8, pp. 253–278, 2005.

[32] M. M. Ali, C. M. Kishtawal, and S. Jain, "Predicting cyclone tracks in the North Indian Ocean: An artificial neural network approach," *Geophys. Res. Lett.*, vol. 34, p. L04 603, Feb. 2007.

[33] I. M. Momin, R. Sharma, and S. Basu, "Satellite-derived heat content in the tropical Indian Ocean," *Remote Sens. Lett.*, vol. 2, no. 4, pp. 269–277, Dec. 2011.

[34] I. F. Pun, I. I. Lin, C. R. Wu, D. S. Ko, and W. T. Liu, "Validation and application of altimetry-derived upper ocean thermal structure in the western North Pacific Ocean for typhoon intensity forecast," *IEEE Trans. Geosci. Remote Sens.*, vol. 45, no. 6, pp. 1616–1630, Jun. 2007.

[35] P. V. Nagamani, M. M. Ali, G. J. Goni, D. Pedro, J. C. Pezzullo, T. V. S. Udaya Bhaskar, V. V. Gopalakrishna, and N. Kurian, "Validation of satellite-derived tropical cyclone heat potential with in situ observations in the North Indian Ocean," *Remote Sens. Lett*, vol. 3, no. 7, pp. 615–620, 2012.